

# ChemComm

Chemical Communications

Accepted Manuscript

This article can be cited before page numbers have been issued, to do this please use: H. Li, H. Fan, R. V. Mahalingam, B. Hu, Y. Feng and J. Song, *Chem. Commun.*, 2020, DOI: 10.1039/D0CC05133K.



This is an Accepted Manuscript, which has been through the Royal Society of Chemistry peer review process and has been accepted for publication.

Accepted Manuscripts are published online shortly after acceptance, before technical editing, formatting and proof reading. Using this free service, authors can make their results available to the community, in citable form, before we publish the edited article. We will replace this Accepted Manuscript with the edited and formatted Advance Article as soon as it is available.

You can find more information about Accepted Manuscripts in the [Information for Authors](#).

Please note that technical editing may introduce minor changes to the text and/or graphics, which may alter content. The journal's standard [Terms & Conditions](#) and the [Ethical guidelines](#) still apply. In no event shall the Royal Society of Chemistry be held responsible for any errors or omissions in this Accepted Manuscript or any consequences arising from the use of any information it contains.

## COMMUNICATION

## A Stable Organic Dye Catholyte for Long-life Aqueous Flow Battery

Hongbin Li, Hao Fan\*, Mahalingam Ravivarma, Bo Hu, Yangyang Feng, Jiangxuan Song\*

Received 00th January 20xx,  
Accepted 00th January 20xx

DOI: 10.1039/x0xx00000x

**An organic dye Basic blue 3 (BB3) was firstly reported as a two-electron catholyte for aqueous redox flow battery. The exceptional stability of BB3 enabled the full battery to achieve high capacity retention of >99.991% per cycle during 1500 cycles.**

Aqueous redox flow batteries (ARFBs) have attracted much attention as one of the most promising large-scale energy storage installations<sup>1-6</sup> due to their independent energy/power deployments, low cost, long-term life, and high safety.<sup>7, 8</sup> Compared to inorganic metal active species such as vanadium<sup>9</sup> and zinc<sup>10</sup> in traditional ARFBs, organic redox-active materials, composed of C, H, O, N and some other Earth-abundant elements, have lower price.<sup>11</sup> Other attractive advantages of organic redox-active materials are their structure diversity and tailorability, which make various benefits such as proper redox potential, fast kinetics, high stability and solubility obtained by researchers through molecules design engineering.<sup>12-15</sup>

To date, organic materials utilized as catholyte for ARFBs are mainly focused on TEMPO,<sup>16-19</sup> ferrocene<sup>20-22</sup> and benzoquinone<sup>23, 24</sup> derivatives. However, they can not meet the actual needs of ARFBs for different reasons. TEMPO and ferrocene derivatives have been exploited as catholyte in neutral environment. Nevertheless, the low ionic conductivity of the anion exchange membrane in neutral electrolyte restricts the rate performance. Moreover, TEMPO derivatives easily occur irreversible side reactions of disproportionation and ring-opening, resulting in severe structural damages.<sup>25</sup> Although benzoquinone has high redox potential, its poor electrochemical stability hinders the application for long-life battery.<sup>23, 24</sup> Therefore, it is urgent to explore organic catholyte materials with high redox potential, attractive solubility and exceptional stability.

Benefited from the  $\pi$ -conjugated structure, aza-substituted basic dyes such as phenazine-based organic molecules exhibit stable electrochemical reversibility.<sup>26-29</sup> However, phenazine-based materials were just used in negative pole due to their low redox potentials. Some researchers have reported a stable phenothiazine-based catholyte with relatively high potential by introducing sulfur atom to the core structure.<sup>29, 30</sup> These work bring great enlightenment to the research of catholyte material. It inspires us that introducing heteroatom atoms such as oxygen family atoms to stabilized  $\pi$ -conjugated structure is an effective way to get a new class of redox active materials with increased redox potential and high stability.

Herein, we reported a highly stable organic dye, Basic blue 3 (BB3), with oxygen atom doped  $\pi$ -conjugated structure, as catholyte for long-life ARFBs. In this work, BB3 was synthesised conveniently through an asymmetric cyclization reaction (Scheme S1, Figure S1). Nitrogen-doped graphene (NG) was introduced to modify the electrode and efficiently reduce the peak separation ( $\Delta E$ ) from 308 to 63 mV in cyclic voltammetry (CV) curves. With acetic acid (HoAc) as cosolvent, the BB3 in H<sub>2</sub>SO<sub>4</sub>-HoAc aqueous solution reached the maximum solubility of 2.5 M, corresponding to the charge capacity of 134 Ah/L. Paired with V<sup>2+</sup>/V<sup>3+</sup> (vanadium) as anolyte, the full battery of BB3/V with NG-modified electrode exhibited a high battery capacity retention of > 99.991% per cycle or > 99.94% per hour during 1500 cycles.

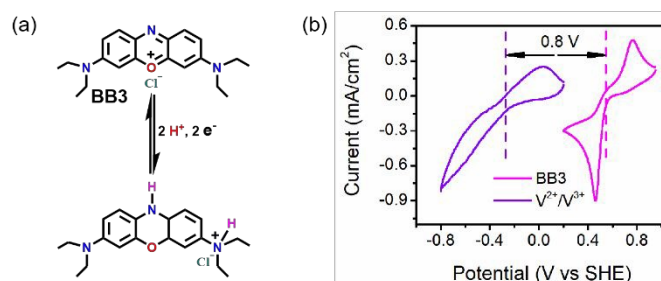


Figure 1. (a) Redox mechanism of BB3. (b) Schematic representation of the full battery of BB3 as cathode paired with V<sup>2+</sup>/V<sup>3+</sup> as anolyte.

State Key Laboratory for Mechanical Behavior of Materials, Shaanxi International Research Center for Soft Matter, Xi'an Jiaotong University, Xi'an 710049, China.

\*E-mail: songjx@xjtu.edu.cn; Fanh2018@xjtu.edu.cn

Electronic Supplementary Information (ESI) available: [details of any supplementary information available should be included here]. See DOI: 10.1039/x0xx00000x

The working principle of the BB3/V ARFB is illustrated in Figure 1. BB3 is one of typical phenoxazinone derivatives, in which three heterocyclic frameworks provide a stably  $\pi$ -conjugated system, and  $p$ - $\pi$  electron donating conjugated effect of two nitrogen atoms makes a steady resonance structure.<sup>31</sup> The heteroatom oxygen increases the electron affinity of the molecules, and thus improves the redox potentials to meet the catholyte demand.<sup>30</sup> The redox reactions of BB3 take place with two electrons and two protons in one step to balance the charge with the extra positive charge locating at the nitrogen atom of the side ammonium group.<sup>32</sup> Compared to single electron transfer molecules, BB3 with two-electron transfers can efficiently improve the battery capacity.

High solubility of the redox active materials is desired to achieve high capacity of the full battery. As calculated via the capacity formula in supporting information, ARFBs with organic electrolyte require an equivalent electron concentration of at least 1.5 M to reach a competitive capacity with all-vanadium ARFBs (~40 Ah/L). In this work, BB3 receives a maximum solubility of 2.5 M in mixed solvent ( $H_2O+HoAc$  volume ratio of 1:1, containing 3.5 M  $H_2SO_4$ ) measured by UV-vis (Figure S2). Considering its ability to store two electrons per molecule, this solubility corresponds to a theoretical equivalent electron concentration of 5.0 M and charge capacity of 134 Ah/L. The high solubility can be attributed to the hydrophilic tertiary amines group at both side chains of BB3. In addition,  $HoAc$  has been demonstrated as a useful cosolvent,<sup>30</sup> which can significantly increase the solubility of BB3. Fourier-transform infrared spectroscopy (FTIR) spectra further proves that there is only some negligible structure change for BB3 in the mixed supporting solution (Figure S3).

CV curve was performed with bare glass carbon (bare GC) electrode in electrochemical workstation to investigate the electrochemical reversibility of BB3. As shown in Figure S4, the redox process of BB3 is acidity dependent due to the protonation/deprotonation of BB3 involved in the redox reaction. The result indicates an apparent CV curve with a redox potential of 0.54 V vs SHE in 3.5 M  $H_2SO_4$  as supporting solution.  $\Delta E$  from CV curve is a useful parameter to estimate the redox dynamics of active species.<sup>33</sup> The CV curve of BB3 with a large  $\Delta E$  reveals sluggish redox kinetics, which might lead to a decrease of energy efficient by creating large over potentials in the full battery.<sup>33, 34</sup>

In order to overcome the drawback of the sluggish kinetics, various nanomaterials have been used to catalyze the redox process of the active species.<sup>35-37</sup> In this work, we introduced NG as an electrocatalyst to modify the bare GC electrode, named as GC@NG. The three-dimensional morphology of NG can supply more active sites for redox reaction (Figure 2a).<sup>38</sup> The high concentration of nitrogen atoms (6.5 at.%, Figure 2b-c) is in favour of superior catalytic activity for the BB3 redox reaction. As shown in Figure 2d, the  $\Delta E$  significantly reduces to 63 mV from 308 mV, indicating a remarkable catalytic effect. Previous work have shown that nanocarbon materials could effectively catalyze the redox process.<sup>39-41</sup> However, in this work, there is no obvious improvement obtained for the BB3 redox process on pure graphene modified bare GC electrode

(Figure S5). Therefore, it is inferred that heteroatom nitrogen plays an important role in the redox process for BB3 on GC@NG.<sup>38</sup>

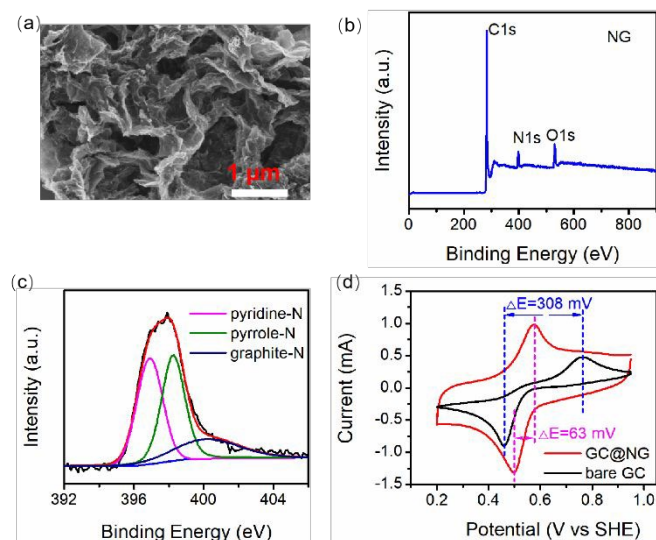


Figure 2. (a) SEM image of the morphology of pure NG. (b) XPS spectrum and (c) N1s high resolution spectra of pure NG. (d) CV curves of 0.05 M BB3 in 3.5 M  $H_2SO_4$  under 0.1 V/s on bare GC and GC@NG, respectively.

The dynamic parameters of BB3 during redox process were measured by linear sweep voltammetry (LSV) on a rotating disk electrode device with the rotations from 400 to 2500 rpm. The LSV curves were obtained by sweeping from the positive to negative potentials on bare GC (Figure S6) and GC@NG (Figure S7) electrodes, respectively. For bare GC electrode, typical sigmoidal LSV curves show one wave at ~0.45 V (Figure S6a), indicating a one-step reaction in the reduction process of BB3. In contrast, GC@NG electrode shows two waves at ~0.40 and ~0.52 V in its LSV curves. The low potential wave is rotation-dependent, representing the reduction process of BB3. The higher one is rotation-independent (Figure S7a-b), suggesting the adsorption process of BB3 on GC@NG, which is further confirmed by the LSV measurements from the reversed sweeping direction (Figure S8). The disappearance of the high potential wave at ~0.52 V in the positive sweeping (Figure S8, S7c-d) could be attributed to the consumption of adsorbed BB3. Clearly, the LSV measurement performed under non-adsorption condition is a better way to determine the diffusion coefficient ( $D_0$ ) and redox constant rate ( $k_0$ ) of redox materials. According to the Levich equation,<sup>33</sup> the  $D_0$  of BB3 in the bulk solution is  $1.1 \times 10^{-7} \text{ cm}^2 \text{ s}^{-1}$ . The redox constant rate  $k_0$  of BB3 on GC@NG calculated through Koutecky-Levich equation is  $2.87 \times 10^{-3} \text{ cm s}^{-1}$ , which is about 1.5 times greater than that on the bare GC electrode ( $1.95 \times 10^{-3} \text{ cm s}^{-1}$ ), revealing that NG effectively facilitates the BB3 redox reaction.

By pairing with  $V^{2+}/V^{3+}$  as anolyte, two BB3/V ARFBs were constructed with 0.05 M BB3 in 3.5 M  $H_2SO_4$  as catholyte using bare carbon paper (bare CP) and NG modified CP (CP@NG) as working electrode, respectively. Compared with bare CP based battery, the CP@NG based battery displays lower overpotentials and higher battery capacity, even at high current densities (Figure 3a, b). Since the resistances of the two

batteries are comparable (Figure S9), the performance difference can be attributed to NG catalyst. The effect of NG on performance is also apparent in the rate capability test (Figure 3c). The Coulombic efficiencies (CE) of two batteries are over 99%. The battery with CP@NG exhibits much better energy efficiency (EE) than that using bare CP (Figure 3d). For example, the CP@NG based battery delivers ~70% EE under 60 mA/cm<sup>2</sup> charge and discharge current density, much higher than that (~40%) of the bare CP based battery. The long-time cycling stability of the 0.05 M BB3/V ARFBs were conducted at 40 mA/cm<sup>2</sup>. The CP@NG based battery exhibits a weak declination in capacity during 1500 cycles testing (Figure 3e). The variation tendency is similar to the battery using bare CP in limited 100 cycles (Figure S10). Therefore, the introduced NG is independent of the battery lifetime. The CP@NG based battery displays high capacity retention of >99.991% per cycle or >99.94% per hour during 1500 cycles, which is outstanding among reported catholytes for ARFBs (Table S1).

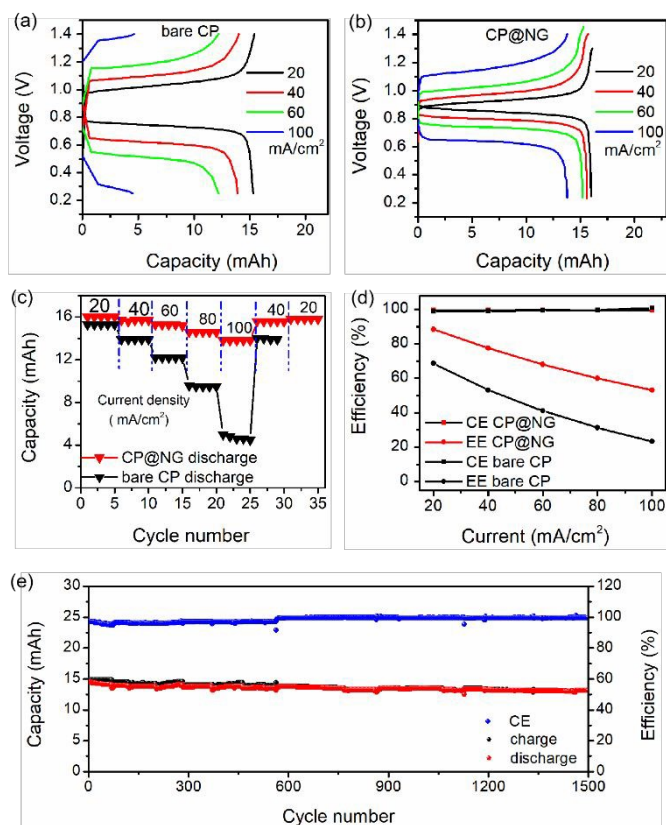


Figure 3. BB3/V ARFBs charge-discharge voltage profiles with catholyte composed of 0.05 M BB3 dissolved in 3.5 M H<sub>2</sub>SO<sub>4</sub> (a) with bare CP and (b) with CP@NG as electrode at different current densities ranging from 20 to 100 mA/cm<sup>2</sup>. Rate capability comparison of bare CP based battery and CP@NG based battery show (c) discharge capacity and (d) EE and CE, respectively. (e) Charge and discharge capacity and CE of the BB3/V ARFB with 0.05 M BB3 using CP@NG as the cathode electrode at 40 mA/cm<sup>2</sup> for 1500 cycles.

The average CE is over 99%, suggesting that the side reaction was negligible and the membrane crossover of the redox species during cycling was at a low rate.<sup>42</sup> CV curve of the post-cycled catholyte shows no obvious peak current loss and redox potential shift relative to the initiate one (Figure S11). In addition, the post-mortem <sup>1</sup>H NMR spectrum exhibits negligibly

slight chemical shift of the specific proton, compared to the initial structure (Figure S12). All the experimental results and analysis prove that the highly soluble BB3 possesses an excellent electrochemical stability for ARFB application. The high stability is mainly attributed to the  $\pi$ -conjugated system provided by the three heterocyclic frameworks of the BB3 core structure. Corresponding proportion capacities are exhibited when the catholyte concentration increases from 0.05 M to 0.5 M and 1.6 M in the full battery test, respectively (Figure S13, S14). That means, the electrochemical process is independent with the solution concentration.

In summary, we firstly reported phenoxazinium derivative BB3 as a promising catholyte for ARFBs. The BB3 exhibits a two-electron, two-proton redox reaction in one step on a redox potential of 0.54 V vs SHE in 3.5 M H<sub>2</sub>SO<sub>4</sub>. The BB3 has a solubility as high as 2.5 M in mixed acid solution, corresponding to the theoretical charge capacity of 134 Ah/L. The exceptional stability of BB3 enables the full BB3/V battery with CP@NG electrode to achieve a high capacity retention of >99.991% per cycle or >99.94% per hour during 1500 cycles, as well as higher energy efficiency and higher battery capacity than those of the cell using bare CP. This work of phenoxazinium derivative utilized as redox-active material will widen the road of the development of organic catholyte material for high performance ARFBs.

## Acknowledgements

This work is financially supported by grants from the National Natural Science Foundation of China (Nos. 21875181 and 51802256), Natural Science Basic Research Program of Shaanxi (Program No.2019JLP-13), Shaanxi Key Research and Development Project (No. 2019TSLGY07-05) and 111 Project 2.0 (BP2018008).

## Conflicts of interest

There are no conflicts to declare.

## Notes and references

1. A. R. Dehghani-Sanij, E. Tharumalingam, M. B. Dusseault and R. Fraser, *Renewable and Sustainable Energy Reviews*, 2019, **104**, 192-208.
2. S. Koohi-Fayegh and M. A. Rosen, *Journal of Energy Storage*, 2020, **27**, 101047
3. Y. Feng, C. Zhang, X. Jiao, Z. Zhou and J. Song, *Energy Storage Materials*, 2020, **25**, 172-179.
4. Q. Liu, Y. Liu, X. Jiao, Z. Song, M. Sadd, X. Xu, A. Matic, S. Xiong and J. Song, *Energy Storage Materials*, 2019, **23**, 105-111.
5. S. Xiong, Y. Liu, P. Jankowski, Q. Liu, F. Nitze, K. Xie, J. Song and A. Matic, *Advanced Functional Materials*, 2020, **30**, 2001444.
6. T. Zhang, Y. Feng, J. Zhang, C. He, D. M. Itkis and J. Song, *Materials Today Nano*, 2020, **12**, 100089.

7. B. Dunn, H. Kamath and J.-M. Tarascon, *Science*, 2011, **334**, 928-935.
8. J. Rugolo and M. J. Aziz, *Energy Environmental Science*, 2012, **5**, 7151-7160.
9. A. Mukhopadhyay, Y. Yang, Y. Li, Y. Chen, H. Li, A. Natan, Y. Liu, D. Cao and H. Zhu, *Advanced Functional Materials*, 2019, **29**, 1903192.
10. D. Chao, W. Zhou, C. Ye, Q. Zhang, Y. Chen, L. Gu, K. Davey and S. Z. Qiao, *Angewandte Chemie International Edition*, 2019, **58**, 7823-7828.
11. P. Poizot, J. Gaubicher, S. Renault, L. Dubois, Y. Liang and Y. Yao, *Chemical Reviewers*, 2020, DOI: 10.1021/acs.chemrev.9b00482.
12. Y. Ding, C. Zhang, L. Zhang, Y. Zhou and G. Yu, *Chemical Society Reviewers*, 2018, **47**, 69-103.
13. Y. Y. Lai, X. Li and Y. Zhu, *ACS Applied Polymer Materials*, 2020, **2**, 113-128.
14. B. Huskinson, M. P. Marshak, C. Suh, S. Er, M. R. Gerhardt, C. J. Galvin, X. Chen, A. Aspuru-Guzik, R. G. Gordon and M. J. Aziz, *Nature*, 2014, **505**, 195-198.
15. K. Lin, Q. Chen, M. R. Gerhardt and L. Tong, *Science*, 2015, **349**, 1529-1532.
16. T. Liu, X. Wei, Z. Nie, V. Sprenkle and W. Wang, *Advanced Energy Materials*, 2016, **6**, 1501449.
17. H. Fan, J. Zhang, R. Mahalingam, J. Song, *ACS Appl. Mater. Interface*, 2020, DOI:10.1021/acsami.0c09941.
18. Y. Liu, M.-A. Goulet, L. Tong, Y. Liu, Y. Ji, L. Wu, R. G. Gordon, M. J. Aziz, Z. Yang and T. Xu, *Chem*, 2019, **5**, 1861-1870.
19. J. Winsberg, T. Janoschka, S. Morgenstern, T. Hagemann, S. Muench, G. Hauffman, J. F. Gohy, M. D. Hager and U. S. Schubert, *Advanced Materials*, 2016, **28**, 2238-2243.
20. B. Hu, C. DeBruler, Z. Rhodes and T. L. Liu, *Journal of the American Chemical Society*, 2017, **139**, 1207-1214.
21. J. Yu, M. Salla, H. Zhang, Y. Ji, F. Zhang, M. Zhou and Q. Wang, *Energy Storage Materials*, 2020, **29**, 216-222.
22. E. S. Beh, D. De Porcellinis, R. L. Gracia, K. T. Xia, R. G. Gordon and M. J. Aziz, *ACS Energy Letters*, 2017, **2**, 639-644.
23. B. Yang, L. Hooper-Burkhardt, F. Wang, G. K. Surya Prakash and S. R. Narayanan, *Journal of The Electrochemical Society*, 2014, **161**, A1371-A1380.
24. P. K. Leung, T. Martin, A. A. Shah, M. A. Anderson and J. Palma, *Chemical Communications*, 2016, **52**, 14270-14273.
25. A. Orita, M. G. Verde, M. Sakai and Y. S. Meng, *Journal of Power Sources*, 2016, **321**, 126-134.
26. A. Hollas, X. Wei, V. Murugesan, Z. Nie, B. Li, D. Reed, J. Liu, V. Sprenkle and W. Wang, *Nature Energy*, 2018, **3**, 508-514.
27. C. de la Cruz, A. Molina, N. Patil, E. Ventosa, R. Marcilla and A. Mavrandonakis, *Sustainable Energy Fuels*, 2020, DOI: 10.1039/d0se00687d.
28. J. Hong and K. Kim, *ChemSusChem*, 2018, **11**, 1866-1872.
29. A. M. Kosswattaarachchi; and T. R. Cook, *ChemElectroChem*, 2018, **5**, 3437-3442.
30. C. Zhang, Z. Niu, S. Peng, Y. Ding, L. Zhang, X. Guo, Y. Zhao and G. Yu, *Advanced Materials*, 2019, **31**, 1901052.
31. J.-F. Ge, C. Arai and M. Ihara, *Dyes and Pigments*, 2008, **79**, 33-39.
32. A. Noorbakhsh, A. Salimi and E. Sharifi, *Electroanalysis*, 2008, **20**, 1788-1797.
33. H. Wang, S. Y. Sayed, E. J. Lubber, B. C. Olsen, S. M. Shirurkar, S. Venkatakrishnan, U. M. Tefashe, A. K. Farquhar, E. S. Smotkin, R. L. McCreery and J. M. Buriak, *ACS Nano*, 2020, **14**, 2575-2584.
34. M. Park, E. S. Beh, E. M. Fell, Y. Jing, E. F. Kerr, D. Porcellinis, M. A. Goulet, J. Ryu, A. A. Wong, R. G. Gordon, J. Cho and M. J. Aziz, *Advanced Energy Materials*, 2019, **9**.
35. Ma, D., Hu, B., Wu, W. et al. Highly active nanostructured CoS<sub>2</sub>/CoS heterojunction electrocatalysts for aqueous polysulfide/iodide redox flow batteries. *Nature Communications* 10, 3367 (2019). <https://doi.org/10.1038/s41467-019-11176-y>
36. Y. Zhu, K. He, T. Tadesse Tsega, N. Ali, J. Zai, S. Huang, X. Qian and Z. Chen, *Sustainable Energy Fuels*, 2020, **4**, 2892-2899.
37. J. Zai, Y. Zhu, K. He, A. Iqbal, S. Huang, Z. Chen and X. Qian, *Materials Chemistry and Physics*, 2020, **250**, 123143.
38. J. Cao, Z. Zhu, J. Xu, M. Tao and Z. Chen, *Journal of Materials Chemistry A*, 2017, **5**, 7944-7951.
39. A. Sodiq, L. Mohapatra, F. Fasmin, S. Mariyam, M. Arunachalam, A. Kheireddine, R. Zaffou and B. Merzougui, *Chemical Communications*, 2019, **55**, 10249-10252.
40. Q. Deng, P. Huang, W.-X. Zhou, Q. Ma, N. Zhou, H. Xie, W. Ling, C.-J. Zhou, Y.-X. Yin, X.-W. Wu, X.-Y. Lu and Y.-G. Guo, *Advanced Energy Materials*, 2017, **7**, 1700461.
41. X. Zhang, Q. Wu, Y. Lv, Y. Li and X. Zhou, *Journal of Materials Chemistry A*, 2019, **7**, 25132-25141.
42. J. Winsberg, T. Hagemann, T. Janoschka, M. D. Hager and U. S. Schubert, *Angewandte Chemie International Edition*, 2017, **56**, 686-711.